Conduction band structure of VSe_2 studied by inverse photoemission, secondary electron emission and total current spectroscopies

1992 J. Phys.: Condens. Matter 4 4075

(http://iopscience.iop.org/0953-8984/4/15/020)

J. Phys.: Condens. Matter 4 (1992) 4075–4082. Printed in the UK

Conduction band structure of VSe_2 studied by inverse photoemission, secondary electron emission and total current spectroscopies

H I Starnberg†, P O Nilsson† and H P Hughes‡

† Department of Physics, Chalmers University of Technology, S-412 96 Göteborg, Sweden
‡ Cavendish Laboratory, Madingley Road, Cambridge CB3 0HE, UK

Received 30 December 1991

Abstract. We have studied the unoccupied electronic states of VSe_2 using three different techniques: inverse photoemission spectroscopy (IPES), secondary electron emission spectroscopy (SEES) and target current spectroscopy (TCS). The experimentally determined electron bands are in good agreement with band structure calculations, but on comparison the different techniques reveal significantly different aspects of the conduction band structure. The reasons for these differences are discussed.

1. Introduction

1.1. Structure and properties of VSe_2

In this paper we report results obtained from VSe_2, which belongs to the family of layered transition metal dichalcogenides (TMDCs). In these compounds, close-packed sheets of metal atoms are sandwiched between sheets of chalcogen atoms. The bonds are strong within each such sandwich, but inter-layer bonds are weak, resulting in remarkably anisotropic properties [1,2]. VSe_2 adopts the so called 1T structure, characterized by octahedrally coordinated metal atoms. The valence bands are derived mainly from the Se 4p orbitals, while the lower conduction bands are primarily of V 3d character. The lowest V 3d band is half-filled, however, which results in metallic properties. Angle-resolved photoemission studies of VSe_2 [3] have produced results in fair agreement with band structure calculations, but a high resolution study revealed that one of the Se 4p derived bands actually crosses the V 3d band and the Fermi level close to the Γ point, giving rise to a small hole pocket [4]. Another important attribute is the appearance of a periodic lattice distortion at temperatures below 110 K [5].

Because of the many interesting phenomena associated with VSe_2, it is a useful test ground for many issues encountered in surface and solid state physics, and an improved understanding of this and related materials is therefore very valuable.

1.2. Methods for conduction band studies

In inverse photoemission spectroscopy (IPES) electrons with well-defined kinetic energy E_{kin} are impinging on the sample surface at an angle θ relative to the surface

0953-8984/92/154075+08$04.50

normal. The electrons undergo dipole transitions to unoccupied states at lower energy, and the emitted photons are detected [6]. In the bremsstrahlung isochromat mode, a band pass filter is used to detect only photons with a certain energy $h\nu$, while E_{kin} is scanned over a certain range.

Secondary electron emission spectroscopy (SEES) can be performed using an ordinary photoelectron spectrometer just by recording the inelastic tail of a photoelectron spectrum. This part of the spectrum is dominated by secondary electrons excited by collisions with photoelectrons, and since the electrons are populating the conduction bands before escaping through the surface barrier, their energy distribution will reflect details of these bands [7, 8]. An electron gun can be used instead of a photon source, since it is unimportant how the energetic electrons, needed for secondary excitations, are produced.

In *target (or total) current spectroscopy* (TCS) *measurements*, an electron beam with fixed kinetic energy is directed onto the sample, which is biased at an adjustable voltage V_b. The total current (or any of its derivatives) through the sample is then measured as a function of V_b. Several mechanisms may be of importance in TCS, but since the elastic reflectance of low-energy electrons depends on the wave-function matching at the surface, the spectra should provide band structure information [9–12].

The aim of this study is twofold: on the one hand we search for more knowledge about the electronic structure of TMDCs; on the other hand we also want to explore how different experimental methods may be used in complementary ways to reveal different aspects of the unoccupied bands.

2. Experimental details

The data were recorded using a VG Scientific ADES 400 system, equipped with a standard gas discharge lamp, a spherical sector electron energy analyzer and a homebuilt IPES unit [13] consisting of a low-energy electron gun and a UV detector with a focusing mirror. The electron energy analyser, which was used for ordinary photoemission spectroscopy as well as SEES, had an angular acceptance of $\pm 2°$ and the energy resolution was typically 0.1 eV. The IPES electron gun produced a 5 μA well-focussed beam, and together with the band-pass detector, operating at $h\nu$ = 9.9 eV, the overall energy resolution was about 0.5 eV. The same electron gun was used also for TCS, but in this mode the beam energy was held constant, apart from the application of a small voltage modulation (0.1 V_{p-p}, 1 kHz); instead, the sample bias was varied, and the first derivative of the target current versus sample bias was registered on a chart recorder, using lock-in detection.

The VSe_2 single crystal was attached to the sample holder by silver filled epoxy resin (Ablebond 84-1LMI), and a clean mirrorlike surface was obtained by cleavage *in situ*. The sample was azimuthally oriented by LEED, and the inequivalent $\overline{\Gamma M}$ and $\overline{\Gamma M'}$ crystallographic directions were identified as described by Law *et al* [14]. The experiments were performed at a base pressure of about 3×10^{-10} Torr, under which conditions the sample surface stayed clean for several weeks, as judged from the absence of any contamination induced features in photoemission spectra.

3. Experimental results

3.1. IPES

Figure 1 shows inverse photoemission spectra measured for four different polar angles of the incident electron beam, in the $\overline{\Gamma M'}$ azimuthal direction. The dominating peaks A and B correspond to the V 3d t_{2g} and e_g bands, respectively, while the weaker structure C has been attributed to an image potential state [15]. Higher conduction bands are seen as rather weak and broad structures (D and F). Other measurements (not shown) were also performed with $\overline{\Gamma M}$ azimuthal orientation.

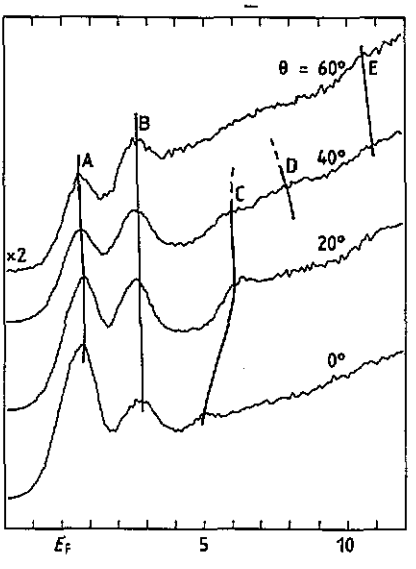

Figure 1. Inverse photoemission spectra of VSe_2 for different polar emission angles θ in the $\overline{\Gamma M'}$ azimuth. The photon energy was 9.9 eV.

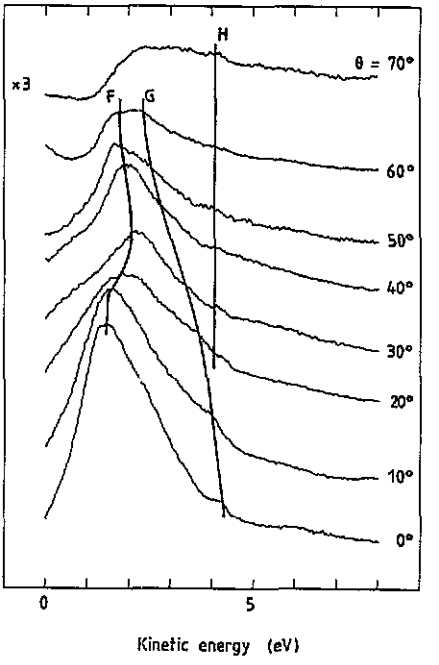

Figure 2. Secondary electron emission spectra of VSe_2 for different polar emission angles θ in the $\overline{\Gamma M'}$ azimuth. The secondary electrons were exited by He I radiation ($h\nu$ = 21.22 eV).

3.2. SEES

Figure 2 shows secondary electron emission spectra excited by He I radiation (21.22 eV). The vacuum level ($E_{kin} = 0$) was determined by the sharp cut-off which appeared in secondary electron emission spectra as the sample was negatively biased (about 5 eV). By measuring the complete spectrum we could obtain the work function Φ = 5.6 eV as the difference between photon energy and total spectral width. The spectra shown in figure 2 were measured without sample biasing, in order to avoid distortion of the angular distribution. The spectra are dominated by one large peak F, which shows significant dispersion with emission angle. In addition there are two tiny peaks, G and H, present, of which H shows very little dispersion. We found that peak H disappeared if Ne I radiation instead was used to excite the electrons. This

indicates that peak H is not a genuine SEES structure, but rather the Se 4s photoemission peak, appearing at a binding energy of about 11 eV, in reasonable agreement with the value calculated by Zunger and Freeman (about 13 eV) [16].

3.3. TCS

Figure 3 shows the derivative of the target current versus the sample bias voltage, with electrons from the IPES gun incident perpendicular to the surface. The peak I corresponds to the onset of current occurring when the incident electrons are retarded precisely to the vacuum level as they reach the sample surface. The bias voltage at the onset corresponds to the effective kinetic energy (corrected for the difference in contact potential between cathode and sample), and serves as an accurate calibration of the electron gun. The features J, K and L in the target current spectrum presumably reflect conduction band edges where the electron reflectivity undergoes rapid changes [9–12].

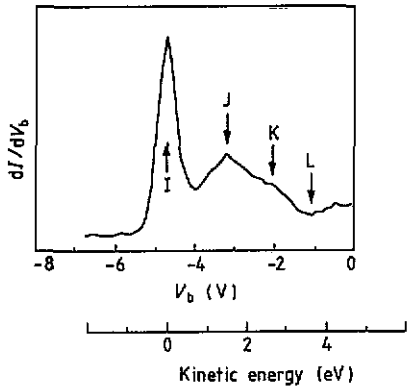

Figure 3. Target current spectrum of VSe_2 showing the first derivative of the target current versus sample bias voltage ($\theta = 0°$). A 5 μA electron beam with $E_{kin} = 4.7$ eV was incident normal to the surface. A scale showing the electronic energies relative to the sample vacuum level has been added.

4. Discussion

From the experimental data it is relatively straightforward to construct structure plots showing initial energy as a function of $k_{||}$, the wave-vector component parallel to the surface.

In IPES the final conduction state energy is simply obtained as

$$E_c = E_{kin} - h\nu. \tag{1}$$

If the energy is to be counted relative to the Fermi level, instead of the vacuum level, one just has to add the work function Φ.

Alternatively one may directly use peak energies relative to the Fermi edge cut-off, as seen in the spectra. The parallel component of the wave vector is given by

$$k_{||} = 0.512\sqrt{E_{kin}}\sin\theta \tag{2}$$

with $k_{||}$ and E_{kin} in units of $Å^{-1}$ and eV, respectively.

In SEES the kinetic energy is equal to the final state energy relative to the vacuum level, and (2) also holds in this case.

Since our TCS spectrum was measured with the electron beam perpendicular to the surface, it corresponds to $k_{||} = 0$. At off-normal electron incidence the sample biasing may alter the value of $k_{||}$, but with suitable experimental design $k_{||}$ can be kept constant, making band mapping along symmetry lines possible [11, 12].

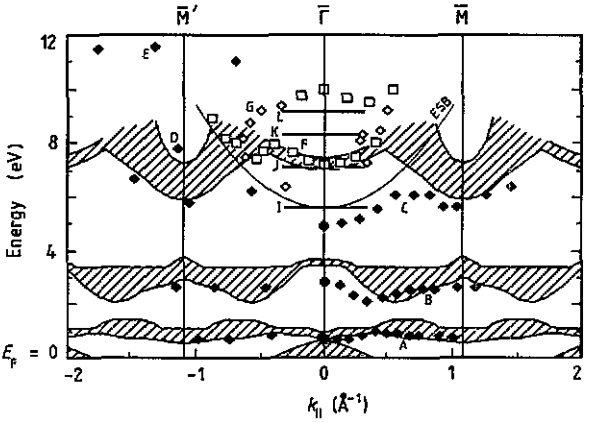

Figure 4. Experimental structure plot showing energy versus $k_{||}$ for different spectral features: (♦) IPES peaks, (□) conspicuous SEES peaks, (◇) weak SEES peaks, (——) TCS features. The effective surface barrier is labelled 'ESB'. The cross-hatched areas represent the two-dimensional projection of the band structure calculated by Zunger and Freeman [16].

Figure 4 compares structure plots for the different experimental techniques with the bands calculated by Zunger and Freeman [16]. Since only $k_{||}$ is determined in the measurements, it is appropriate to compare the experimental structure plots with the projection of the three-dimensional band structure onto the surface Brillouin zone. We have constructed such a surface projection by cross-hatching the areas between bands calculated along the ΓM and AL symmetry lines. Since calculated bands are not available for more general k points, we have neglected that some bands may have extremal points not located on the ΓM and AL lines. Such details are not likely to affect our comparison with experiments significantly. As mentioned above, Φ was determined from the total width of photoelectron spectra at 21.22 eV photon energy, which positions the vacuum level relative to E_F. The parabola seen in the middle of figure 4 is the effective surface barrier for escaping free electrons, given by $E = \Phi + 3.81(k_{||})^2$, with energies in eV and wave vector in $Å^{-1}$. Of the three techniques used, only IPES can provide results below this barrier.

The IPES data points, shown as filled squares, were positioned on the energy scale according to (1). Accurate calibration of the IPES gun was offered by the TCS measurement, using the fact that the surface peak (I in figure 3) appears when the kinetic energy (eV) equals the negative sample bias (V). The IPES results are in good agreement with those published by other groups [14, 15]. Comparing peaks A and B with the calculated t_{2g} and e_g bands, it is clear that the latter should be shifted down by about 0.2 and 0.7 eV, respectively. The lowest V 3d band, which should be partially unoccupied for $k_{||} \approx 0$, is not resolved in the spectra, but for $k_{||}$ in the

range ± 0.3 Å $^{-1}$ the peak A data points appear somewhat closer to E_F; this could well be due to contributions from that band. The hole pocket around Γ, induced by a highly dispersive Se 4p band, is not observed, which is quite natural given the modest resolution of the IPES and the overlap with V 3d bands of higher transition probability. Peak C has been attributed to an image potential state [15] because of its parabolic dispersion and because it is located in a calculated band gap; its location relative to the effective surface barrier supports that view, but its sensitivity to work function changes should be further studied before a firm designation can be made. The weak and broad structures D and E at higher energies are due to transitions into bands predominantly of V 4s and 4p character [14]. Comparison with calculations are unfortunately not possible, since those available do not extend up to these energies.

The SEES data, which are shown as unfilled squares in figure 4, provide a different view of the conduction band structure. The theory of this technique is less developed than that of IPES and ordinary photoemission, and there are uncertainties about how to interpret SEES peaks. The simplest approach is to associate SEES peaks with maxima in the one-dimensional density of states, i.e. the density of states along lines of constant $k_{||}$ in k space. Band mapping is very simple in this case: the energies relative to the vacuum level are obtained directly from the spectra, while $k_{||}$ is given by (2). The spectral features should also be affected by the population dynamics of the conduction bands. Electrons may, for example, accumulate at band minima through repeated interactions with phonons, or a dominant de-excitation channel may preferentially populate a particular conduction band state. Mack *et al* [8] concluded, in a study of the Ir(111) surface, that the group velocity of the band states also influenced the energy distribution of secondary electrons. In practice, however, conduction bands have been mapped in good agreement with calculated bands, without corrections for such effects [7, 17]. As can be seen in figure 4, the simple mapping approach applied for peak F yields excellent agreement with the calculated lowest V 4s–4p band. This may partly be attributed to the quasi two-dimensional nature of this band, which leaves little room for lineshape distortions. One higher band or edge is indicated by peak G, but present calculations do not allow for any comparison. It should be pointed out that some data points close to the effective surface barrier may be artefacts produced by the associated cut-off.

As our TCS investigation was limited to normal incidence of the electron beam, it produced only data for $k_{||} = 0$. In order to be clearly visible, they are shown as horizontal bars in figure 4, but their lengths have no physical significance. The data points were adjusted vertically to align peak I with the vacuum level. The theory of TCS, which has been examined by Komolov and Chatterton [9], involves a multitude of mechanisms associated with both elastic and inelastic reflection of electrons at the surface. Of particular importance for the elastic contribution to TCS is the matching at the surface of external free-electron states to internal conduction band states. TCS shares this aspect with SEES, which to some extent can be considered as inverse TCS, although modulated by the population dynamics. At band edges we expect to see rapid changes in the target current, reflecting the changes in the density of available states for the incoming electrons to populate. In target current spectra like that in figure 3 (first derivative), lower band edges should result in peaks, while the upper edges should produce minima. Using the second derivative, as done by Schaefer *et al* [18], one would instead expect peaks and valleys to appear between the band edges together with additional structure generated by the derivation. For bands with negligible dispersion along $k_\perp$ that may be appropriate, but generally we expect that

the first derivative is more straightforward to interpret. It should be pointed out that even in first-derivative spectra, peaks and valleys may appear slightly displaced from the corresponding critical points, but Strocov [11, 12] has recently devised a correction procedure, involving simple LEED type calculations, that makes accurate band mapping by TCS possible. In figure 4 we notice that peak J, which is the most prominent TCS band signature, appears in excellent agreement with both the calculated V 4s/4p band edge and the SEES data. The next peak K and the valley L may correspond to the lower and upper edge of the next band, but these features are weaker and presumably less straightforward to interpret. Calculated bands are again unavailable at these energies and the SEES data do not correlate favourably with these features.

5. Conclusions

We have found that our experimental results on the conduction band structure of VSe_2, obtained by IPES, SEES and TCS, are in good qualitative agreement with the bands calculated by Zunger and Freeman [16]. The agreement is excellent for the V 4s/4p bands, located about 7.5 eV above E_F, and by shifting the calculated V 3d bands down by about 0.2 eV (t_{2g}) and about 0.7 eV (e_g), good agreement is found also for these. To advance the understanding of the VSe_2 electronic structure further, there is an urgent need for band calculations that extend to higher energies than the existing ones.

We have also established that a combination of different electron spectroscopies can be very fruitful, in that such offers complementary views of the conduction bands.

IPES is likely to remain the most important method for studies of unoccupied bands, since it is theoretically well understood and since it is the only technique of the three that gives access to the important part of the unoccupied band structure located below the effective surface barrier. One drawback of IPES is that the sensitivity for bands of s and p character is quite low at the photon energies commonly used.

One serious limitation in SEES is the tendency of relevant band signatures to appear only as weak shoulders on a large and sloping background. It is therefore important to strive for good statistics, and the use of derivatives and background subtraction may also help to improve the situation. For better accuracy it is also desirable to develop the theory of SEES further. Among the merits of SEES we must stress that it can, because of its different selection rules, provide vital information about bands that are practically invisible to IPES. Since the measurements can be done with equipment that is almost ubiquitous in surface science laboratories, it should be routinely done to supplement IPES measurements.

In addition, TCS is attractive for conduction band studies because of its experimental simplicity and the modest cost involved. It presumably shares with SEES the sensitivity to many conduction band details that are difficult to detect in IPES, and used in combination with relatively simple calculation schemes it may become the foremost technique for mapping of higher bands [11, 12]. Continued progress in theoretical understanding of TCS may enhance the power of this technique even further.

Acknowledgments

This work was supported by The Swedish Research Council for Natural Science. We

are also grateful to L Ilver for assistance with the IPES measurements and to Dr A R Law for valuable discussions.

References

[1] Wilson J A and Yoffe A D 1969 *Adv. Phys.* **18** 193
[2] Friend R H and Yoffe A D 1987 *Adv. Phys.* **36** 1
[3] Johnson M T, Starnberg H I and Hughes H P 1986 *J. Phys. C: Solid State Phys.* **19** L451
[4] Skibowski M 1991 *Landolt-Börnstein New Series* III/23b ed A Goldmann and E-E Koch (Berlin: Springer)
[5] Williams P M 1976 *Crystallography and Crystal Chemistry of Materials with Layered Structures* ed F Lévy (Dordrecht: Reidel) pp 51–92
[6] Smith N V 1988 *Rep. Prog. Phys.* **51** 1227
[7] Zimmer H-G, Westphal D, Kleinherbers K K, Goldmann A and Richard A 1984 *Surf. Sci.* **146** 425
[8] Mack J U, Bertel E, Netzer F P and Lloyd D R 1986 *Z. Phys.* B **63** 97
[9] Komolov S A and Chadderton L T 1979 *Surf. Sci.* **90** 359
[10] Jaklevic R C and Davis L C 1982 *Phys. Rev.* B **26** 5391
[11] Strocov V N 1991 *Solid State Commun.* **78** 545; 1992 *Phys. Status Solidi* b **169** 115
[12] Strocov V N and Komolov S A 1991 *Phys. Status Solidi* b **167** 605
[13] Ilver L 1992 to be published
[14] Law A R, Andrews P T and Hughes H P 1991 *J. Phys.: Condens. Matter* **3** 813
[15] Claessen R, Schäfer I and Skibowski M 1990 *J. Phys.: Condens. Matter* **2** 10045
[16] Zunger A and Freeman A J 1979 *Phys. Rev.* B **19** 6001
[17] Maeda F, Takahashi T, Ohsawa H, Suzuki S and Suematsu H 1988 *Phys. Rev.* B **37** 4482
[18] Schäfer I, Schlüter M and Skibowski M 1987 *Phys. Rev.* B **35** 7663